

Dear Revisors,

We would like to thank you for your encouraging comments, which we largely agree upon. We are sure that the manuscript will greatly benefit from your suggestions. Hereafter the list of your comments is reported, followed by our response. We will also provide a version of the manuscript with the tracked revisions.

Referee #2 comments: The English in which this paper is written is awkward in places, although comprehensible, and the authors should use shorter paragraphs. The title of the paper is misconceived. It is not a study of emergency management but a description of the deployment and use of a landslide monitoring and alarm system.

Authors: The manuscript was revised by a native English speaker, and the paragraphs were shortened.

Referee #2: The title of the paper is misconceived. It is not a study of emergency management but a description of the deployment and use of a landslide monitoring and alarm system.

Authors: The title was changed as suggested into:

"GB-InSAR monitoring of slope deformations in a mountainous area affected by debris flow events"

Referee #2: Line 9: Deep Seated Gravitational Slope Deformation - as it is not a common noun and adjectives, this term should not be capitalised. The same issue occurs with other terminology.

Line 33: have been increasingly being recognized - adjust, please

Line 79: Jurassic

Line 90: please do not use contractions in formal prose.

Figure 3 includes wording that will not reproduce at the page scale. it should be redrafted.

Authors: all of the further referee minor corrections were accepted, and the legend of figure 3 was improved.

Kindest regards

William T. Fisher

~~Emergency management of the 2010 Mt. Rotolon landslide by means of a local scale GB-InSAR monitoring system~~

"GB-InSAR monitoring of slope deformations in a mountainous area affected by debris flow events"

William Frodella¹, Teresa Salvatici¹, Veronica Pazzi¹, Stefano Morelli¹, Riccardo Fanti¹

1. Department of Earth Sciences, University of Firenze, Via La Pira 4, 50121, Florence, Italy

Correspondence to: William Frodella (william.frodella@unifi.it)

Abstract

Diffuse and severe slope instabilities affected the whole Veneto region (Northeast Italy) between October 31st and November 2nd 2010, following a period of heavy and persistent rainfall. In this context on November 4th 2010 a large detrital mass detached from the cover of the Mt. Rotolon ~~dDeep sSeated gGravitational sSlope dDeformation~~ (DSGSD), located in the upper Agno River Valley, channelizing within the Rotolon Creek riverbed and evolving into a highly mobile debris flow. The latter phenomena damaged many hydraulic works, also ~~threatening putting at high risk~~ bridges, local roads, together with ~~population the residents~~ of the Maltaure, Turcati and Parlati villages located along the creek banks and ~~of~~ the Recoaro Terme town. ~~Starting-Fr~~ From the beginning of the emergency phase, the Civil Protection system was activated, involving the National Civil Protection Department, Veneto Region, ~~and local administrations~~ personnel and technicians, as well as scientific institutions. On December 8th 2010 a local scale monitoring system, based on a ~~gGround bBased iInterferometric sSynthetic aAperture rRadar~~ (GB-InSAR), was implemented in order to evaluate the slope deformation pattern evolution in correspondence of the debris flow detachment sector, with the final aim of assessing the landslide residual risk and manage the emergency phase. This paper describes the ~~resultsouteomes~~ of a two years GB-InSAR monitoring campaign (December 2010 - December 2012), its application for monitoring, mapping, and emergency management activities, in order to provide a rapid and easy communication of the results to the involved technicians and civil protection personnel, for a better understanding of the landslide phenomena and ~~the~~ decision-making process in a critical landslide scenario.

1 Introduction

Deep ~~sSeated gGravitational sSlope dDeformations~~ (DSGSD) are normally not considered hazardous phenomena, due to their typically very slow evolution; nevertheless under certain conditions ground movements can accelerate evolving into faster mass movements, ~~which may favour-or favoring~~ collateral landslide processes (Crosta, 1996; Crosta and Agliardi, 2003). Therefore, a multidisciplinary approach is fundamental in order to understand the complex nature of such phenomena, ~~so as towith the aim of~~ assessing the correct mitigation measures. In this framework advanced mapping methods, based on spaceborne, aerial and terrestrial remote sensing platforms, represent the optimal solution for landslide detection, monitoring and mapping, in ~~variousdifferent~~ physiographic and land cover conditions, ~~with special-regardsparticularly withto~~ large phenomena and hazardous non accessible sectors (Casagli, 2017b; Guzzetti et al., 2012). In ~~recentthe last~~ decades, many advanced remote sensing technologies have ~~gained widespread recognitionbeen increasingly being recognized~~ as efficient remote surveying techniques for the characterization, and

monitoring of landslide-affected areas, in terms of resolution, accuracy, data visualization, management, and reproducibility. ~~Among these are, such as:~~ digital photogrammetry (Chandler, 1999; Zhang et al., 2004), laser scanning (Abellan et al., 2006; Gigli et al., 2012, 2014c; Jaboyedoff et al., 2012; Tapete et al., 2012), Infrared Thermography (Teza et al., 2012; Gigli et al. 2014a, b; Frodella et al., 2015) and radar interferometry, both terrestrial and satellite (Luzi et al., 2004; Bardi et al., 2014; Tofani et al., 2014; Ciampalini et al., 2016; Gullà et al., 2017; Peduto et al., 2017a).

Ground ~~b~~Based ~~i~~nterferometric ~~s~~ynthetic ~~a~~perture ~~r~~adar (GB-InSAR) systems in particular, for their ~~e~~apability ~~to~~of measuring displacements with high geometric accuracy, temporal sampling frequency, and adaptability to specific applications (Monserrat et al., 2014), represent powerful devices successfully employed in: a) engineering and geological applications for detecting structural deformation, and surface ground displacements (Tarchi et al., 1997; 2003; Antonello et al., 2004; Casagli et al., 2010; 2017a), b) for the monitoring of volcanic activity (Nolesini et al., 2013; Di Traglia et al., 2014a, b), ~~and~~ c) for analysing the stability of historical towns built on isolated hilltops (Luzi et al., 2004; Frodella et al., 2016; Nolesini et al., 2016). Furthermore, in ~~the~~ recent years GB-InSAR technique has developed to an extent where it can significantly contribute to the management of major technical and environmental disasters (Del Ventisette et al., 2011; Broussolle et al., 2014; Lombardi et al., 2017; Bardi et al., 2017a, b). Between October 31st 2010 and November 2nd 2010 the whole Veneto region territory (north-eastern Italy; Fig. 1) was hit by heavy and persistent rainfall, that ~~diffusely~~ triggered widespread floodings and abundant slope failures, causing extensivewidespread damages to people (3 fatalities and about 3500 evacuated people) and structures., not to mention furthermore resulting in heavy economic losses inforthe agricultural, livestock, and industrial activities.

In this context on November 4th 2010, part of detrital cover of the Rotolon DSGSD suffered the detachment of a mass approximately 320000 m³ in volume, thatwhich channelized in the Rotolon Creek bed causing a large debris flow. This phenomenon was characterized by more than three kilometres of run-out-~~distance~~, damaging various hydraulic works ~~and infrastructures~~ (creek dams, weirs, bank protections), and threatening putting at high risk the various structuresinfrastructures (bridges, local roads, houses); together with ~~the population of the inhabited areas located nearby the creek banks (those residing in the~~ villages of Maltaure, Turcati, Parlati and the town of Recoaro Terme; Fig. 1).

On December 8th 2010 a GB-InSAR monitoring system was implemented in order to assess the landslide residual displacements and support the local authorities infor the emergency management (Fidolini et al., 2015), calling into play. In this framework the Civil Protection system was activated in order to manage the landslide emergency phase, by involving the both the national (DPC) and regional (DPCR) ~~c~~Civil ~~p~~rotection ~~d~~epartments, in cooperation with scientific institutions (namely “~~c~~Competence centres”, CdCs), local administration personnel, and technicians (Bertolaso et al., 2009; Pagliara et al., 2014; Ciampalini et al., 2015). Accurate geomorphological field surveys were also carried out in this phase, in order to analyse the landslide morphological features ands to improve the radar data interpretation (Frodella et al., 2014; 2015; 2017). In addition, a 3D landslide ~~3D~~ runout numerical modelling was performed towith the aim of identifying the source and impact areas of potentialssible debris flow events-source and impacted areas, flow velocity and deposit distribution within the Rotolon creek valley (Salvatici et al., 2017).

This workpaper is focused on the outcomes-results of a long-term continuous GB-InSAR monitoring campaign (December 2010 - December 2012) carried out during the post-event recovery phase, in which monitoring, mapping, and emergency management activities were implemented tofor assessing the landslide residual risk and analyse its kinematics. In this contextframework field activities were carried out by local Civil Protection operators and technicians for a validation of the remotely sensed data (landslide area inspections). In particular, the analysed radar data were

shared with the ~~involved~~ technicians and civil protection personnel ~~involved~~ in order to provide a rapid and easy communication of the results, and enhance the synergy ~~of with~~ all ~~of~~ the subjects involved in the recovery phase.

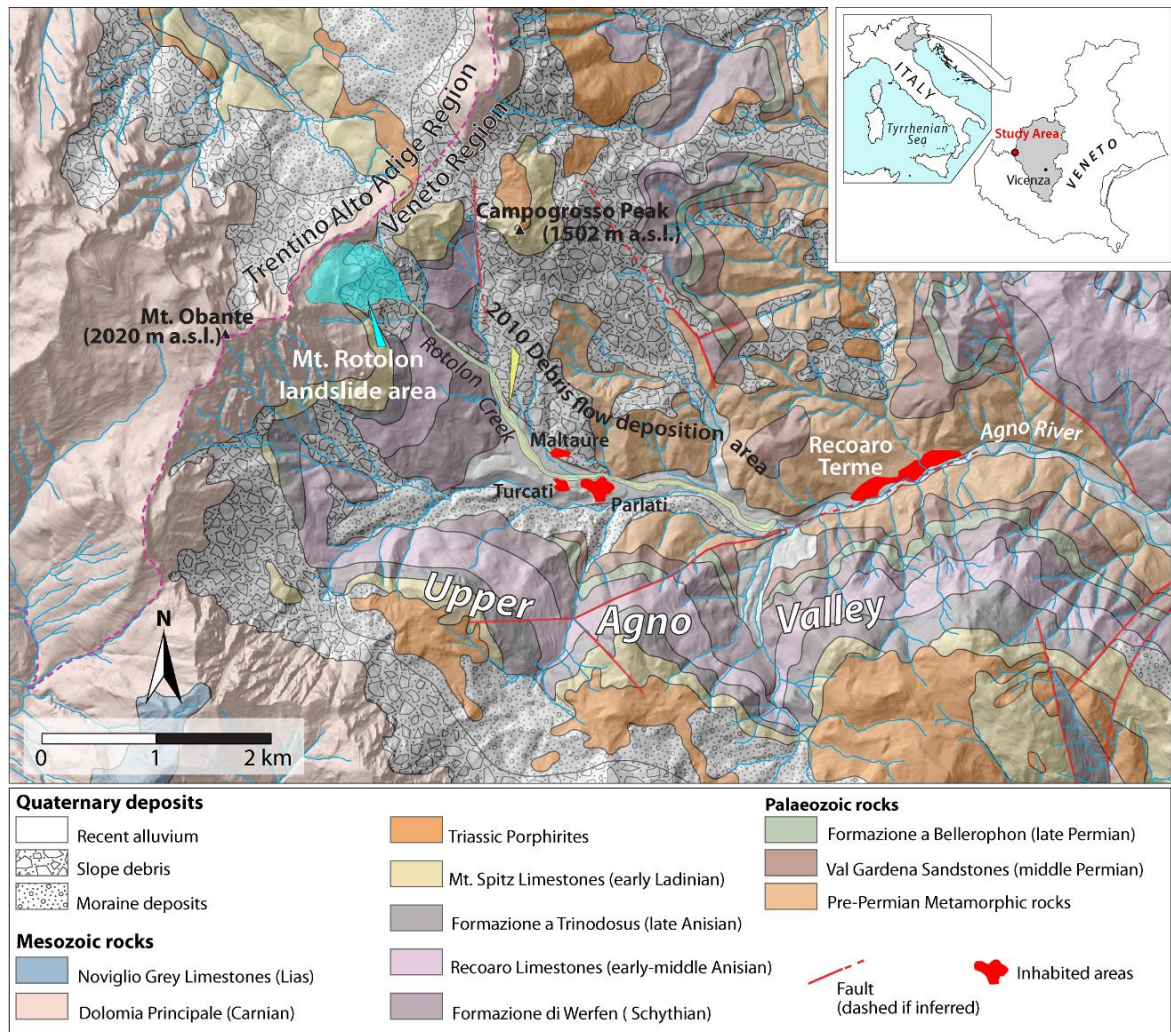
108

2. Study area

The Rotolon DSGSD is located in the Vicentine Prealps, on the south-eastern flank of the Little Dolomites chain, in the uppermost Agno river valley (Fig. 1). The instability processes of the ~~area valley~~, such as slope failures and debris flows induced as secondary phenomena of the DSGSD, have threatened the ~~u~~Upper Agno valley for centuries (Frodella et al., 2014).

From a geological point of view the landslide develops in the uppermost portion of a ~~mainly dolomitic-limestone stratigraphic succession~~, sub-horizontally bedded ~~mainly dolomitic limestone stratigraphic succession~~, from middle Triassic to lower ~~JG~~ Jurassic in age, belonging to the South Alpine Domain (De Zanche and Mietto, 1981).

117



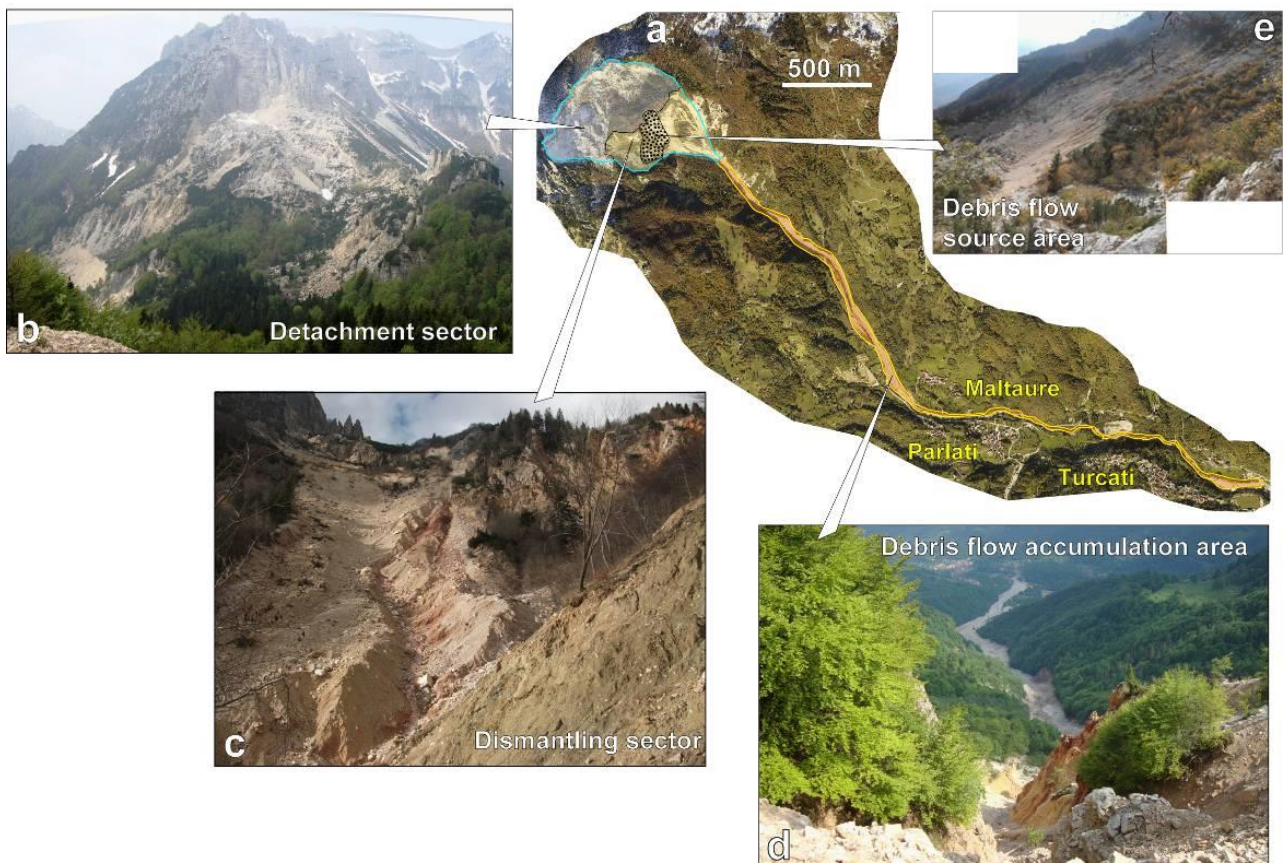
118

Figure 1. Geological sketch map of the Upper Agno River Valley with the location of the Rotolon landslide.

The mass movement is delimited to the NW by the ridge of the Mount Obante group and develops from about 1700 to 1100 m a.s.l., covering an area of 448000 m². The Rotolon DSGSD can be classified as a DSGSD (“~~s~~Sackung type”; Zischinsky, 1969), and ~~it is~~ characterized by a complex activity (Cruden and Varnes, 1996) ~~causing that leads to~~ a rough ~~morphology physiographic, characterized by with~~ steep scarps, trenches, crests and counterscarps (Figs. 2 and 3).

123

124 Two distinct sectors can be identified, baseding on the acting dominant slope instability processes in act: i) an upper
 125 “~~d~~Detachment sector”, followed downstream by a ii) “~~d~~Dismantling sector” (Frodella et al., 2014). The ~~d~~Detachment
 126 sector (~~with~~having a mean slope of 30°), develops downstream ~~efrom~~ the main landslide crown (Figs. 2a and b; Fig. 3),
 127 and ~~it~~is dominated by extensional deformation ~~causingthat leads to~~ the development of tensional fractures, resulting in
 128 alternate trenches and crests ~~creatingwhich creates a~~ very rough, stepped topographic surface. This area is affected ~~both~~
 129 by gravitational and erosional processes, ~~as well asand by~~ the rock mass detensioning and disaggregation, ~~resulting~~
 130 ~~inwhich cause~~ the accumulation of various depositional elements (colluvial fans, colluvial aprons, rock fall and rock
 131 avalanche deposits) formed by very coarse ~~and~~ heterometric clasts, ranging from cobbles to boulders with scattered
 132 blocks (decimetric to decametric in size) in a coarse sandy matrix (Figs. 3 and 4).
 133 The ~~d~~Dismantling ~~sector-area~~ (mean slope of 34°) includes sectors formed by ~~sub-vertical~~highly weathered ~~sub-vertical~~
 134 rock walls. It is dominated by surf~~ace~~icial processes (e.g., concentrated and diffuse erosion, slope-waste deposition due
 135 to gravity, detrital cover failures) that ~~widely-substantially~~ cover the evidences of deeper deformations (Figs. 3 and 4).
 136 ~~This areae Dismantling sector~~supplies material for debris flows, which channelize downstream within the Rotolon
 137 ~~c~~Creek bed, ~~therefore~~representing the most critical sector ~~forwith respect to~~ short-term hazardous phenomena.
 138



139
 140 **Figure 2.** The Mt. Rotolon DSGSD plan (a); landslide sectors (b, c) and the 2010 debris flow features (d, e).

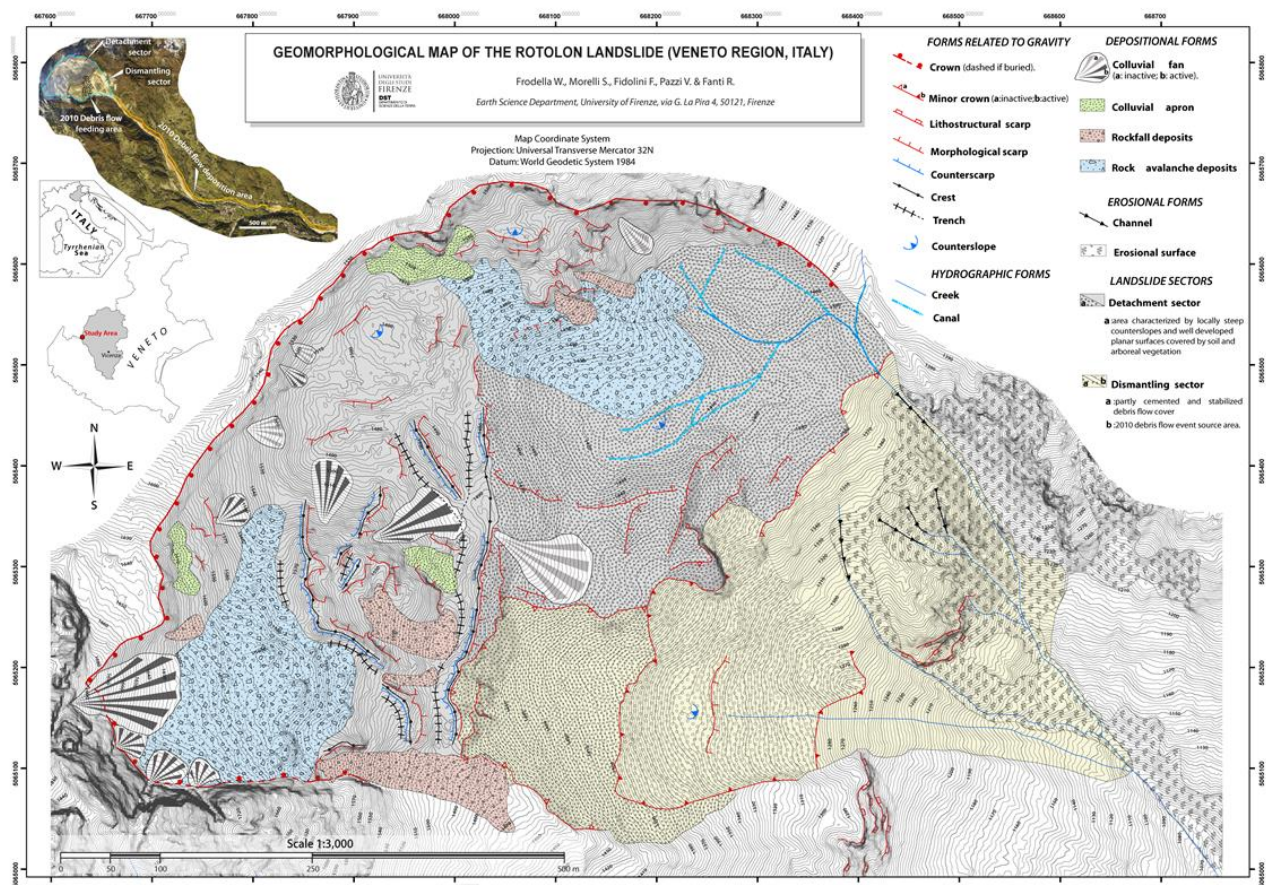


Figure 3. Geomorphological map of the Rotolon Landslide (modified after Frodella et al., 2014).

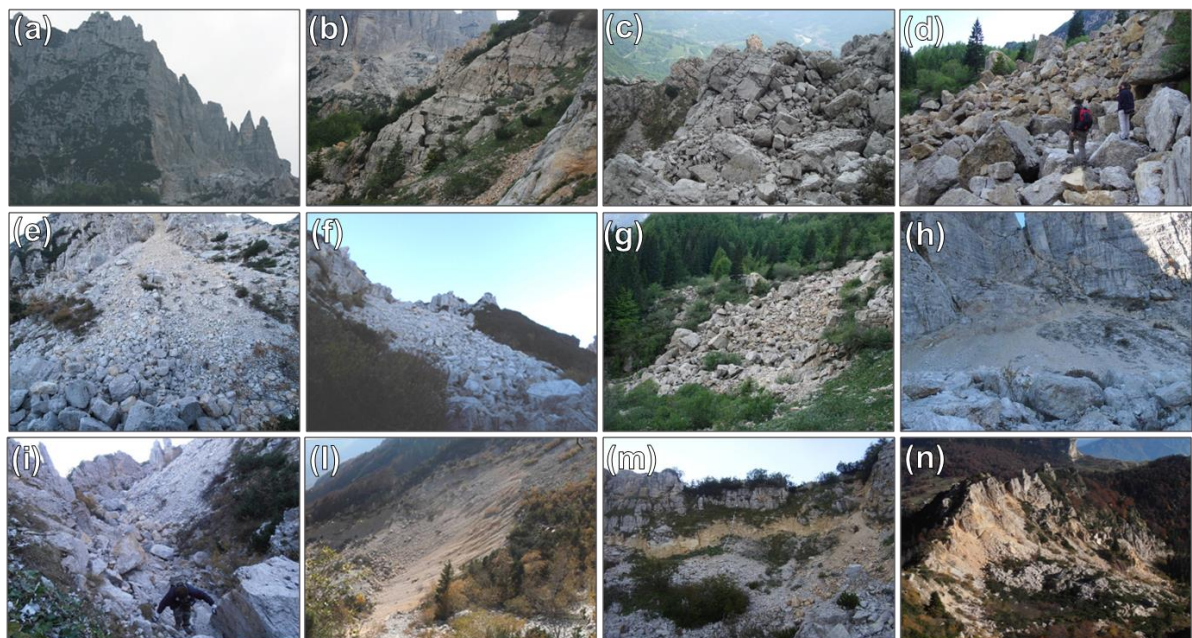


Figure 4. Geomorphic and sedimentary features of the Mt. Rotolon DSGSD: **(a)** rock walls prone to rock falls; **(b, c)** rock mass affected by different stages of disaggregation; **(d)** plurimetric rock blocks within rock avalanche deposit. Main depositional elements within the landslide body: **(e)** colluvial fan; **(f, g)** channelized and diffused rock fall deposits; **(h)** colluvial aprons. Main landslide linear elements: **(i)** landslide trench; **(l)** 2010 debris flow detachment scarp; **(m)** DSGSD crown sector; **(n)** landslide crest.

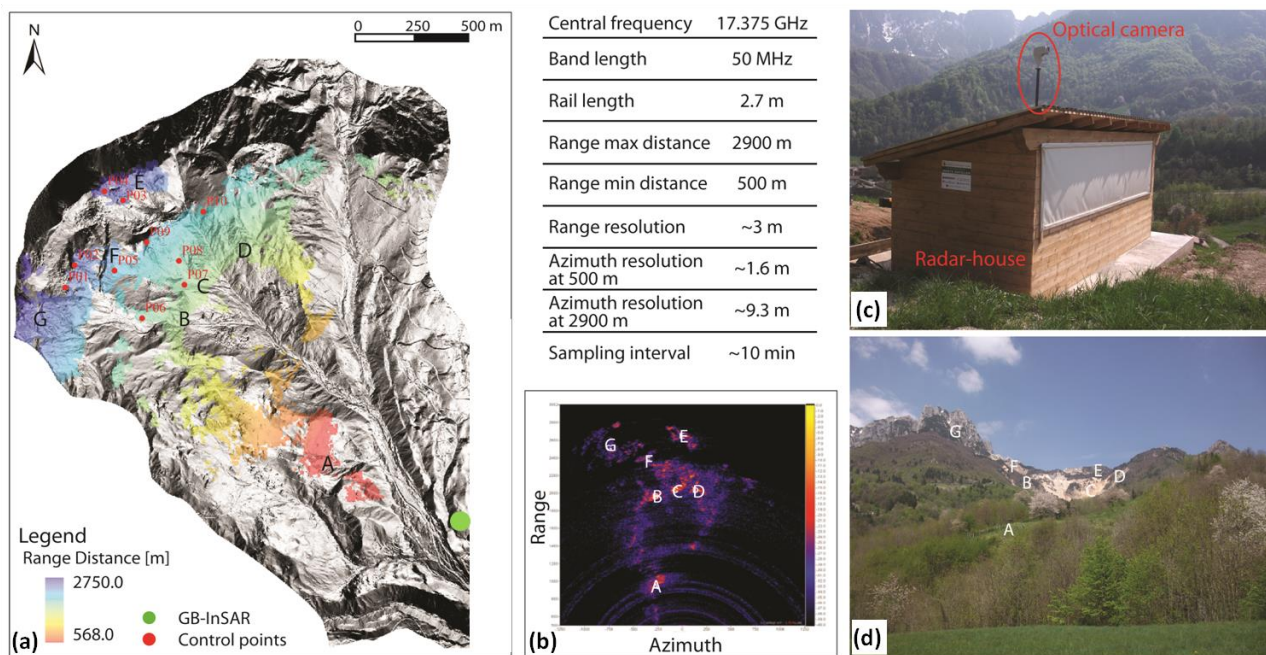
3. The GB-InSAR technique basic theoretical principles

The GB-InSAR is a computer-controlled microwave transmitting and receiving antenna, that moves along a mechanical linear rail in order to synthesize a linear aperture along the azimuth direction (Tarchi et al., 1997). ~~The device~~ radiates ~~an area with~~ microwaves in the Ku band (12-18 GHz) and registers the backscattered signal in the acquiring time interval (~~from few to~~ less than 1 minute with the most modern systems). Each acquisition produces a complex matrix of values from which phase and amplitude information are calculated (Luzi et al., 2004; Luzi, 2010). A SAR image contains amplitude and phase information of the observed objects' backscattered echo within the investigated scenario, and it is obtained by combining the spatial resolution along the direction perpendicular to the rail (range resolution, ΔR_r) and the one parallel to the synthetic aperture (azimuth or cross-range resolution, ΔR_{az}) (Luzi, 2010). The working principle of the GB-InSAR technique is the evaluation of the phase difference, pixel by pixel, between two pairs of averaged sequential SAR complex images, which ~~form~~~~constitutes~~ an interferogram (Bamler and Hartl, 1998). The latter does not contain topographic information, given the antennas fixed position during different scans (zero baseline condition). Therefore, in the elapsed time between the acquisition of two or more subsequent coherent SAR images, it is possible to derive from the obtained interferograms a 2D map of the displacements that occurred along the sensor LOS (~~with a millimeter accuracy in the Ku band~~) (Tarchi et al., 1997; 2003; Pieraccini et al., 2000; 2002). The capability of InSAR to detect ground displacement depends on the persistence of phase coherence (ranging from 0 to 1) over appropriate time intervals (Luzi, 2010). Among the technique's advantages ~~it should be highlighted it must be noted~~ that GB-InSAR works: a) without any physical contact with the slope, avoiding the need of accessing the area; b) in almost ~~every~~~~any~~ light and atmospheric condition; c) continuously over a long time; d) with ~~a~~~~millimetric~~~~ice~~ accuracy ~~(the accuracy of the measured phase is usually a fraction of the operated wavelength; Luzi, 2010)~~; e) providing ~~extensive and detailed~~ near real time ~~detailed and spatially extensive~~ information.

This latter feature in particular gives a strong advantage with respect to traditional ground surface methods (like inclinometers, extensometers, total stations), which on the contrary provide single-point information, ~~and are~~ generally ~~are~~ not sufficient to evaluate the kinematics and ~~potential~~ behaviour of ~~a~~ complex landslide. The main drawback of the technique is the logistics of the installation platform, both because the GB-InSAR system measures only the displacement component parallel to the line of sight (L.O.S.), and because the azimuth resolution (the ability to separate two objects perpendicular to the distance between the sensor and the target) ~~lessens~~~~reduces~~ with the increase of the distance ~~with respect to~~~~from~~ the target (Fig. 5). Moreover, vegetated areas can be another drawback of the technique since they are commonly characterized by ~~signal~~ low coherence and power intensity.

4. The adopted monitoring system

The GB-InSAR system was installed in the Maltaure village, at an average distance of 3 km ~~with respect to~~~~from~~ the landslide, pointing upwards to NW (Fig. 5). The radar parameters are summarized in Fig. 5. Given the acquisition setting of the site and the civil protection ~~needs~~~~purposes~~, the radar data covers an area of 1.2 km². The logistics of the GB-InSAR system installation favored a good spatial coverage of the data on the monitored area, especially with ~~special~~ regards to the ~~d~~~~D~~ismantling sector. Nevertheless, shadowing effects, due to the slope roughness, crests and counter-slope surfaces affect the ~~d~~~~D~~etachment sectors (Figs. 5 and 7).



185
186 **Figure 5.** The adopted monitoring system: (a) Location of the GB-InSAR system and radar data coverage features (A-
187 G=recognized landslide sectors); (b) the adopted monitoring parameters and radar power image, displaying the
188 correspondent recognized landslide sectors; (c) the radar system hut setting; (d) picture of the monitoring optical system
189 scenario (A-G=corresponding sectors).

190 The radar system acquired GB-InSAR data every 10 minutes, from which cumulated 2D displacement maps, and
191 displacements time series of 10 measuring points (Fig. 5) were obtained. GB-InSAR data were processed using
192 LiSALab software (Ellegi s.r.l.) and uploaded via LAN network: i) on a dedicated Web-based interface, allowing for a
193 near real time data on-routine visualization; ii) on a remote ftp server (in ASCII format), in order to perform on demand
194 analysis in case of critical weather events forecast bybased on the national civil protection weather forecast system (Fig.
195 6). The latter were performed integrating into a GIS environment the displacement maps and comparing them with
196 ancillary data (rainfall, geological and geomorphological maps). In addition, a remotely adjustable robotized high
197 resolution optical camera (Ulisse Compact model produced by Videotec S.p.A, digital zoom 10x - 36x),
198 manouverableageable via IP-Ethernet interface, was installed in correspondence withof the radar system, acquiring data
199 every 60 minutes and allowing for programmable zooms. The objective of this device waswith the aim ofto checking of
200 the landslide-hazardous and inaccessible Dismantling sector of the landslide (Figs. 5 and 6). The time line rationale of
201 the monitoring system and emergency management procedures is summarized in Fig. 6.

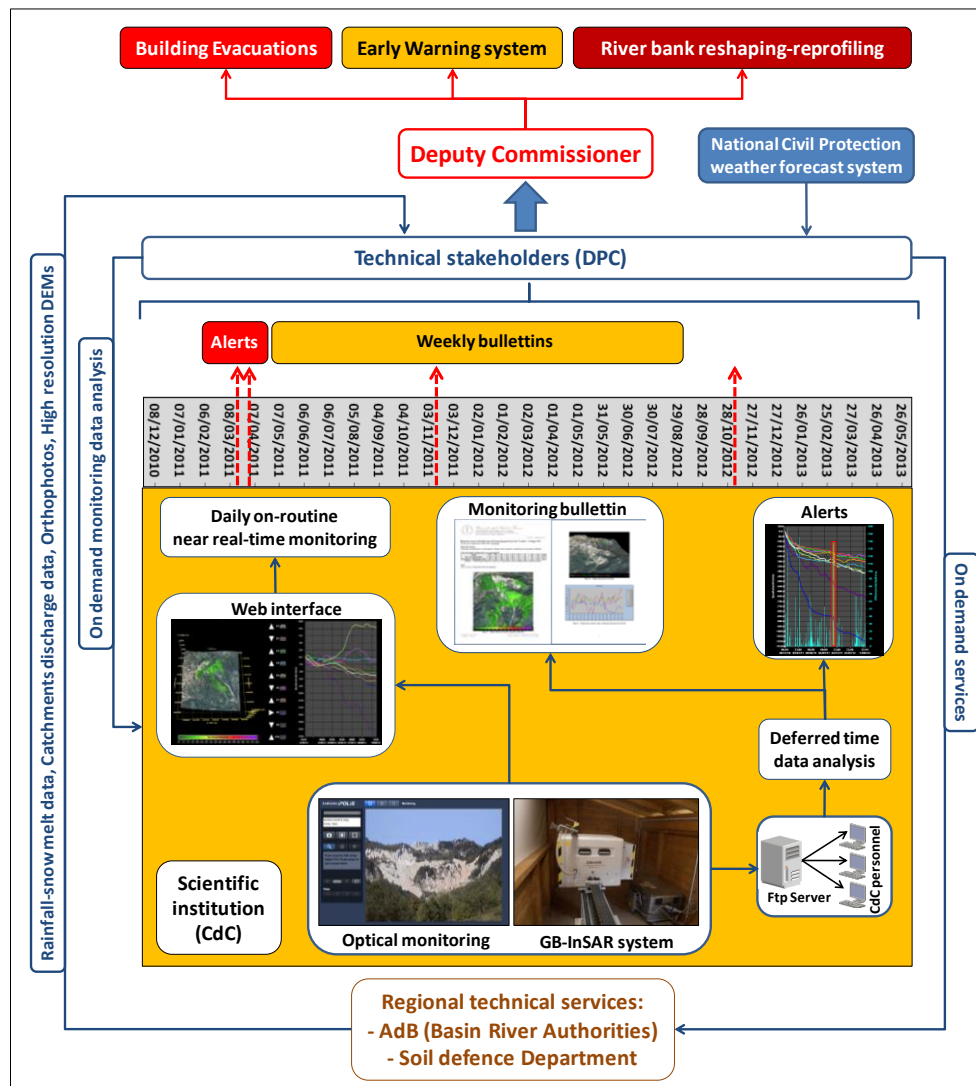


Figure 6. Time line rationale of the Rotolon monitoring system and emergency management procedures.

5. GB-InSAR data analysis

The obtained GB-InSAR incremental cumulative displacement (ICD) maps and the displacement time series of the measuring points obtained displacement time series are shown in Figs. 7 and 8, respectively. By using a selected colour scale, the obtained radar maps obtained are displayed as a function of the displacement measured in the period covered by the acquisitions, spanning from December 8th 2010 up to the beginning of each month of the monitoring campaign, until the end of the monitoring period (the negative displacement values indicate movements approaching to the sensor; Fig. 7). In order to evaluate the deformation rates and provide an easily-interpretable data, a traffic light-type colour scale was applied in all the displacement maps.

GB-InSAR measuring points (corresponding to a 5 x 5 pixel size area) were selected in correspondence with sectors where the radar signal is characterized by high stability, in order to monitor the landslide kinematics and characterize the various landslide physiographic features (Fig. 7). Furthermore with the aim of performing a temporally detailed displacement analysis and detecting the spatial pattern of residual landslide deformation, monthly cumulated displacement (MCD) maps were also selected and analysed from the collected GB-InSAR dataset (Fig. 9).

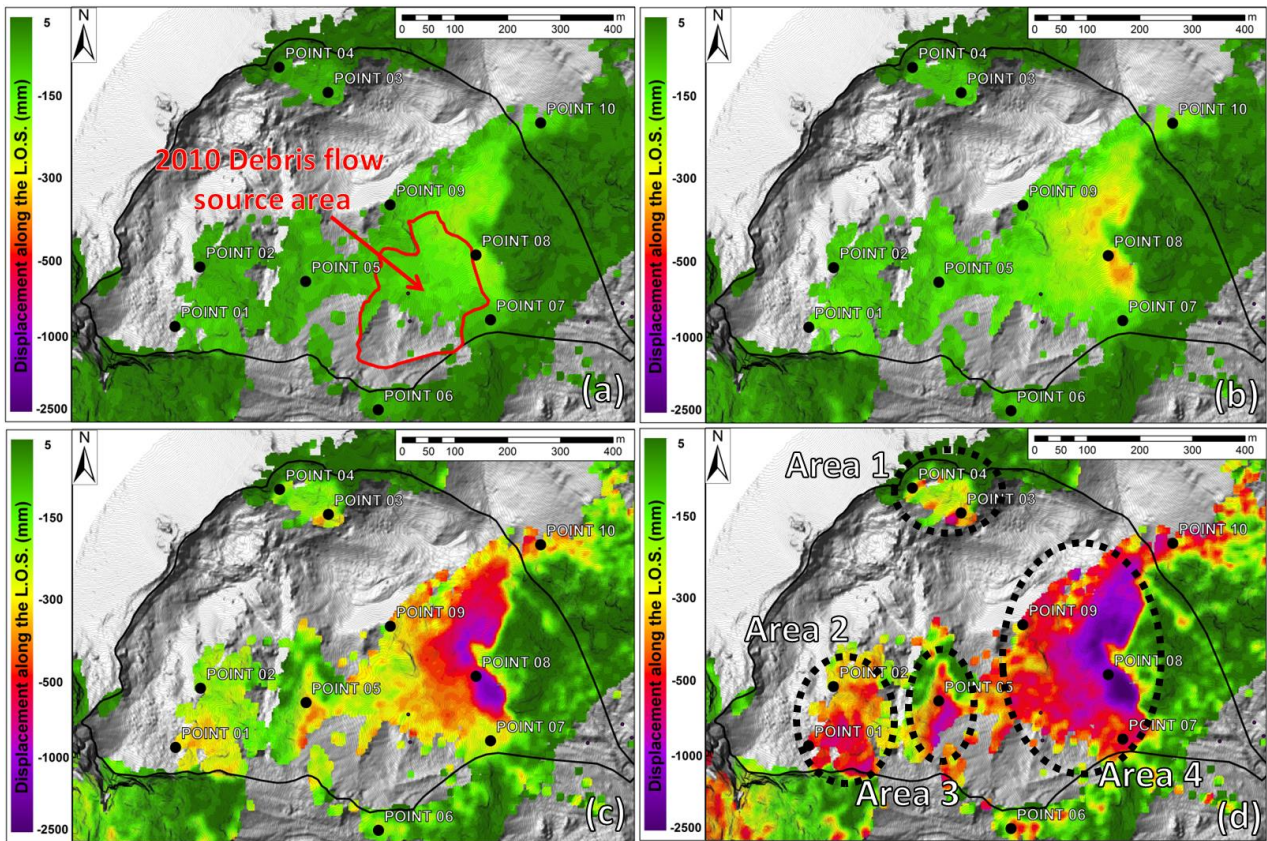


Figure 7. ICD maps of the Rotolon landslide: (a) December 8th 2010 - January 1st 2011; (b) December 8th 2010 - February 1st 2011; (c) December 8th 2010 - December 1st 2011; (d) December 8th 2010 - December 31st 2012 (Point 1-10 represent the GB-InSAR measurement points in correspondence of which the displacement time series were extracted).

From the analysis of the collected GB-InSAR dataset of the ICD maps (Fig. 7) four distinct areas characterized by relevant residual cumulated displacement were identified (Fig. 7d):

- Area 1 (ICD=737 mm, about 12500 m² in extension) and Area 2 (ICD=751 mm, area of 28000 m²), corresponding to the material infilling the **d**Detachment sector (Fig. 2), such as minor rock fall and rock avalanche deposits;
- Area 3 (ICD=960 mm; 12000 m² in extension) and Area 4 (ICD=2437 mm; 88000 m² coverage), both falling within the **d**Dismantling sector detrital cover (Fig. 2) which was not affected by the 2010 debris flow detachment.

The measuring points time series (Fig. 8) display cumulated displacements ranging from 337 mm (Point 6) to 595 mm (Point 4, located in Area 1); Point 8 in particular (falling within Area 4) displays the monitored area cumulated peak displacements (ICD=1476 mm), showing two acceleration periods (middle March 2011 and beginning of November 2011), alternating with a more linear trend. The comparison amongst the MCD maps highlighted a first phase of widespread residual displacements (December 2010, Fig. 9a), which gradually decreased **starting** from the following month (Fig. 9b). In the **subsequentfollowing** period ground deformation took place in correspondence **with** limited sectors within Area 4 (May 2011 in particular shows **the** higher MCD up to 244 mm; Fig. 9d), except for a widespread reactivation recorded in November 2011 (Fig. 9e).

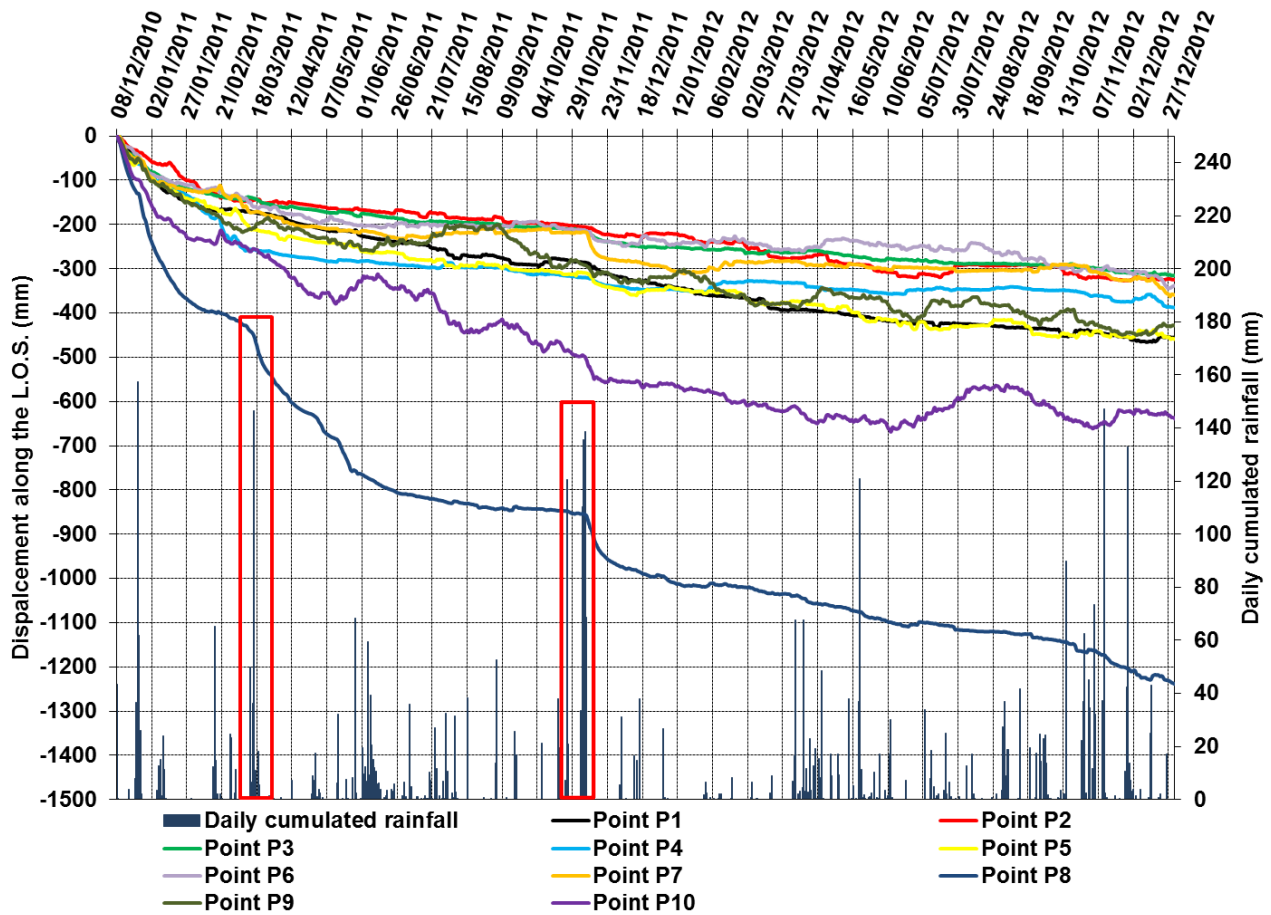


Figure 8. Selected measuring points displacement time series of the monitored scenario (red squares enhance Point 8 accelerations).

Furthermore, in order to automatically extract the most hazardous residual displacement sectors, the MCD dataset was analysed by means of a MATLAB code (Salvatici et al., 2017) (Fig. 10). The code extracts from the dataset all of the areas affected by deformation higher than a selected threshold value, set equal to 92.3 mm, being the minimum displacement among all the maximum MCD values. The results are displacement maps showing only the areas with such selected displacements (Fig.10 a-d), confirming the trend highlighted by the MCD maps (Fig. 9). The second operation of the employed code consists in the frequency calculation of the displacement occurred (the code computes how many times each pixel has recorded the selected displacement during the monitoring period) (Fig. 10e). By using this method, three critical areas characterized by repeated residual reactivations were detected: Area 2, Area 3 (1 reactivation) and especially Area 4 (8 reactivations).

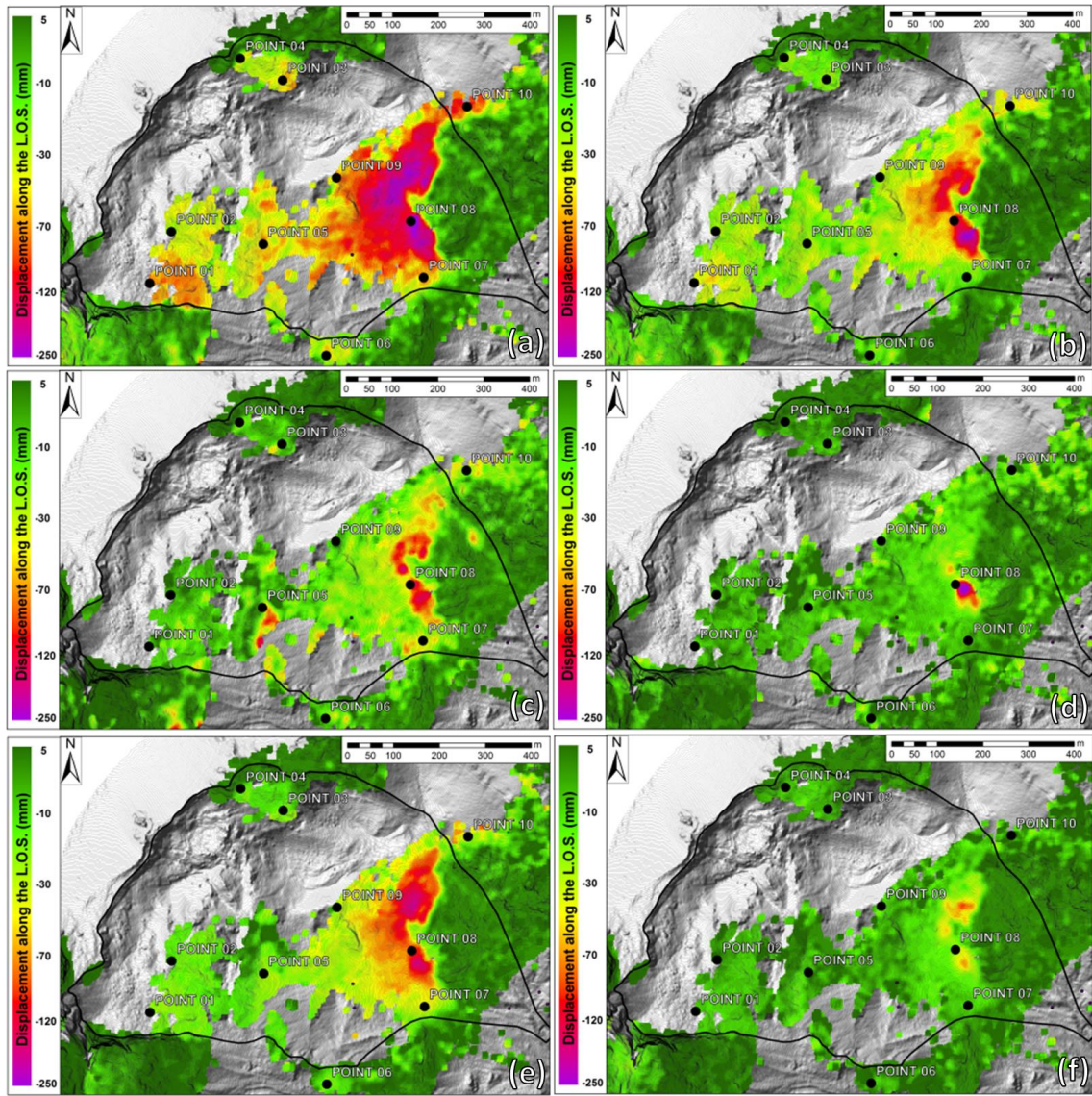


Figure 9. Selection of MCD maps from the GB-InSAR dataset: (a) December 2010 (232 mm cumulated peak displacement); (b) January 2011 (214 mm); (c) March 2011 (173 mm); (d) May 2011 (244 mm); (e) November 2011 (174 mm); (f) November 2012 (106 mm).

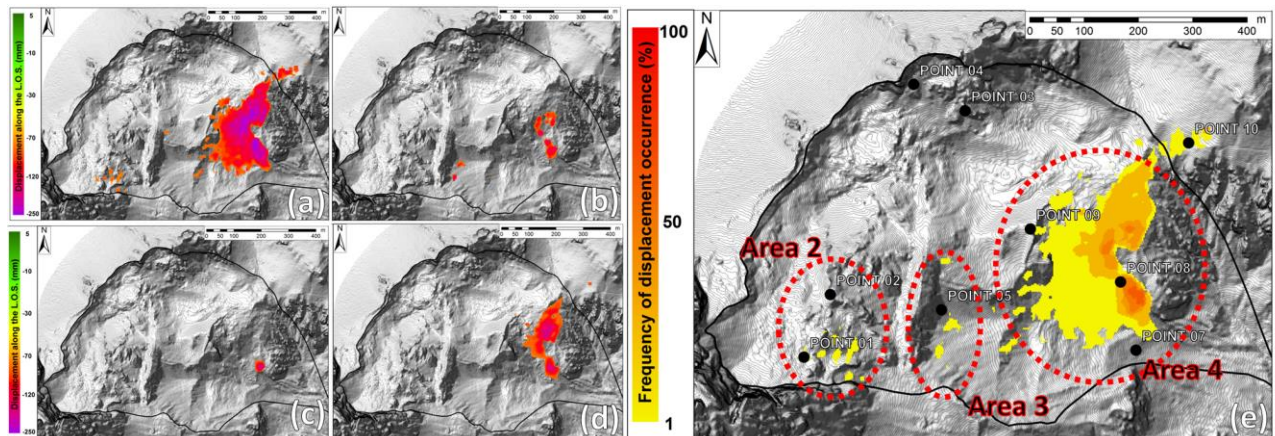


Figure 10. Residual reactivation maps obtained from selected MCD maps by means of the employed MATLAB code analysis: (a) December 2010; (b) March 2011; (c) May 2011; (d) November 2011; (e) frequency map of the reactivation of the critical residual displacement sectors, classified based on their activation frequency.

6. Discussion

Successful strategies for landslide residual hazard assessment and risk reduction would imply integrated methodologies for instability detection, mapping, monitoring, and forecasting (Confuorto et al., 2017). In order to provide information on the nature, extent and activation frequency of ancient landslides, standard detection and mapping procedures need a combination of field-based studies and advanced techniques, such as remote sensing data analysis and geophysical investigations (Ciampalini et al., 2015; Lotti et al., 2015; Del Soldato et al., 2016; Morelli et al., 2017; Pazzi et al., 2017a, b). In this context, GB-InSAR represents a versatile and flexible technology, allowing for rapid changes in the type of data acquisition (geometry and temporal sampling) based on the characteristics of the monitored slope failure, which is capable of assessing the extent and the magnitude of the landslide residual hazard (Di Traglia et al., 2014; 2015; Carlà et al., 2016a, b). In the presented case study the 2 year continuous GB-InSAR monitoring campaign made it possible to measure the slope displacement with a millimetric accuracy over a 1.2 km square landslide area, enabling the analyses of the evolution pattern connected to the landslide residual hazard. The measured deformation pattern is consistent, in terms of extent and values, with the results obtained by an automated total station monitoring network, working approximately in parallel with the GB-InSAR system (Frigerio et al., 2014; Bossi et al., 2015).

By comparing the landslide geomorphological map (Frodella et al., 2014) with the ICD displacement map of whole monitored period (Fig. 11), the four critical areas shown in Figure 7 are analysed in detail:

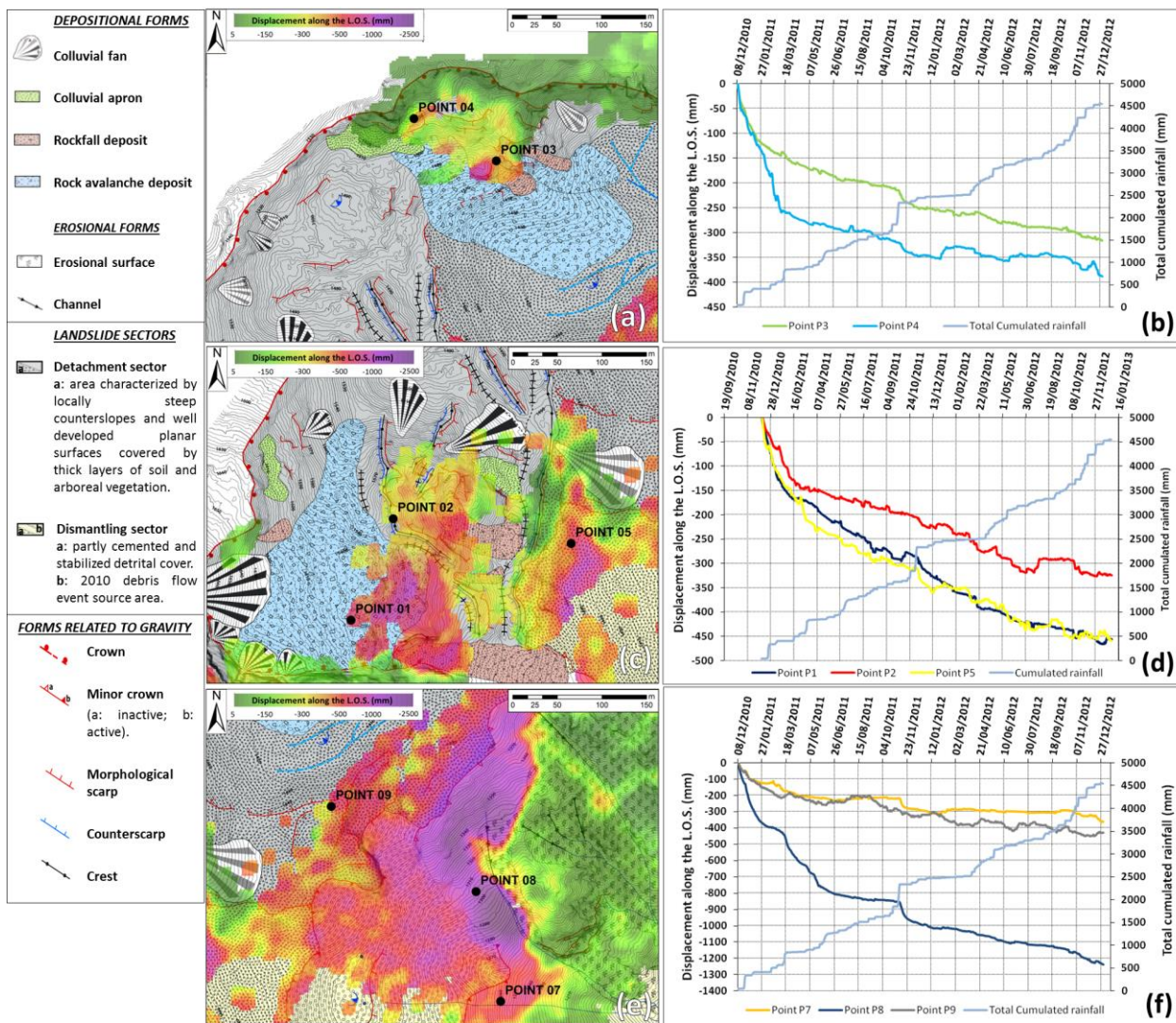
- Area 1, including measuring Points 3 and 4, is located in the northern side of the Detachment sector (Fig. 11a). In the first few months (between December 2010 and March 2011) the points recorded in the first few months (between December 2010 and March 2011), a peak of displacements of about 260 mm (Point 4) and 150 mm (Point 3); after this period the displacement decreased up to 8th November 2011. Between November 8th and 12th November, during a major rainfall event (68 mm), the displacements increased again (Fig. 11b). The displacements recorded by the points within Area 1 may be related to deformations affecting the deposits placed along the steep scarp connected to the main crown delimiting the DSGSD (Fig. 4).

- Area 2 is located in the Detachment sector (SW side of the DSGSD). Two measuring points (Points 1 and 2) therein located (Fig. 11d) recorded a peak of displacement between December 2010 and March 2011 of about 170 mm (Point 1) and 130 mm (Point 2), respectively, between December 2010 and March 2011. The ground deformations recorded by these points are related to slope waste deposition due to the gravity affecting the coarse material infilling this sector, such as ancient rock avalanche deposits (Point 1) and detensioned rock mass portions (Point 2) (Fig. 4).

- Area 3 represents the border between Detachment and Dismantling sectors, and is located upstream of the 2010 event scarp (Fig. 11c). Its kinematics is represented by Point 5 behaviour, showing a trend similar to P1, which may be associated with the sliding of the partly cemented and stabilized detrital cover material infilling the materials, showing a similar trend with respect to P1 (Figs. 4-11d).

- Area 4 represents the lowermost portion of Dismantling sector. Three measuring points are therein located: Points 7, 8 and 9 (Figs. 11e and 11f). Points 7 and 8 display the kinematics the detrital cover surrounding the 2010 debris flow triggering area. Both control points show acceleration periods alternating with periods of stability. In particular the trend of P8, located near the Rotolon creek ephemeral springs and channels (Frodella et al., 2014; 2015) shows a correlation with cumulative precipitation above a threshold value of about 100 mm (Fig. 11f), which contribute to the sub-surface water circulation within the detachment sector's loose detrital cover.

295 This suggests that the recorded displacements may be associated to the spring erosion within the detrital cover. This
 296 point records the maximum displacement of the entire area (about ICD=1236 mm) monitored by GB-InSAR system-~~of~~
 297 about ICD=1236 mm. The area ~~it~~ is apparently dominated by superficial processes, such as widespread soil erosion and
 298 slope-waste deposition due to gravity. Measuring Point 9, located near~~by~~ the ~~d~~Dismantling sector upstream limit,
 299 records cumulative displacement of 445 mm and shows an irregular trend mainly due to its location near vegetated
 300 areas (Figs. 4-119f).
 301



302
 303 **Figure 11.** Integration between geomorphological map (modified after Frodella et al., 2014), the ICD maps
 304 displacement maps of whole monitored period, and the control points displacements time series: (a) the zoom of the
 305 Area 1 shown in Figure 7d; (b) the displacements time series of P4 and P3; (c) zoom of the Area 2 and Area 3 shown in
 306 Figure 7d; (d) the displacement time series of Points 1, 2 and 5; (e) zoom of Area 4 shown in Figure 7d; (f) the
 307 displacement time series of Points 7, 8 and 9.

308 The use of GB-InSAR ICD maps and the integration with geomorphological field surveys proved its usefulness in
 309 recognizing Area 4 (located within the DSGSD ~~d~~Dismantling sector; Figs. 3 and 7) as the most hazardous sector within
 310 the monitored scenario, due to the widespread and intense recorded cumulated displacements (2437 mm), and its

geomorphological features (steep slope, loose very coarse debris and ~~acting widespread~~ surface ~~widespread~~ erosional processes ~~in act~~ due to the presence of ephemeral springs), and frequency of reactivations (Fig. 10).

The main triggering factor for ~~these shallow remobilizations ongoing in~~ this area ~~shallow remobilizations are~~ intense rainfall events, as highlighted by measuring point 8 time series (Fig. 8). Area 3 (recording 960 mm of total cumulated displacements) falls as well within the Dismantling sector detrital cover, and was considered the second most hazardous landslide sector within the monitored scenario.

Other areas characterized by relevant residual cumulated displacement were identified in Area 1 (737 mm) and Area 2 (751 mm), corresponding to the material infilling the Detachment sector (Fig. 2), but they were not considered hazardous due to a 300 meter long and 20 meter high N-S trending trench acting as a physical barrier separating the upper ~~d~~Detachment sector from the lowermost ~~d~~Dismantling sector.

Furthermore the comparison amongst the MCD maps (Fig. 9 and 10) highlighted widespread and frequent residual displacements taking place in ~~correspondence of~~ Area 4 during the wet ~~autumn-winter-fall~~ months (December 2010=232 mm; January 2011=214 mm; March 2011=173 mm; November 2011, 2012=174 and 106 mm respectively). Nevertheless, in May 2011 Area 4 reached the highest MCD in the monitored period (244 mm), although concentrated in a limited sector located near ~~by~~ the measuring Point 8 (Fig. 9d).

A simplified local scale early warning system (Intrieri et al., 2012) was implemented based on three different warning levels: ordinary, pre-alarm and alarm levels (Figure 5). In order to ensure the safety ~~offor~~ the post-recovery management personnel, hourly displacement thresholds were adopted: the level change occurred if the following thresholds were surpassed (i) ~~ordinary: <1 mm/h-ordinary~~; ii) ~~pre-alarm: between 1.0 mm/h to and 5.0 mm/h-for the pre-~~alarm; iii) ~~alarm level: >5 mm/h-for the alarm level~~). Communication, which is a fundamental issue of every early warning system (Intrieri et al. 2013), was operated through the dispatch of monitoring bulletins every week and whenever the warning thresholds were exceeded. In this framework, based on the surface of the deformation areas and the increasing trends of displacement time series, 4 monitoring alerts were obtained: i) March 19th 2011; ii) April 7th 2011; iii) 8-12th November 2011; iv) November 10-12th 2012 (Fig. 6). All these events were located in the area monitored by measuring Point 8. Inspections carried out by the optical monitoring device and by means of field surveys from safe viewing points, assessed that ~~the~~ detected accelerations did not generate significant slope failures, although rainfall comparable to that of November 2010 had hit the area. Following the second alert, a weekly bulletin phase (May 2011 - September 2012) was planned for a residual risk prevention strategy.

7. Conclusions

In the ~~framework context~~ of the 2010 hazardous events affecting the Rotolon creek valley, a local scale GB-InSAR system was implemented for: i) mapping and monitoring slope landslide residual deformations; ~~and for ii)~~ early warning purposes in case of landslide reactivations. ~~The objective, with the aim of was to~~ assuring the safety of ~~both~~ the valley's inhabitants and the personnel involved in the post-event recovery phase. The radar system acquired GB-InSAR data every 10 minutes, from which cumulated 2D displacement maps, and displacements time series of 10 measuring points were obtained. The analysed GB-InSAR data were uploaded both on a dedicated Web-based interface and remote ftp server, allowing for: i) a daily near real time ~~data and~~ on-routine ~~data~~ visualization; ii) ~~and~~ on demand analysis in case of critical weather events. In this ~~context framework~~, based on the surface of the deformation areas and the increasing trends of displacement time series, 4 monitoring alerts were obtained and a 16 months weekly monitoring bulletin campaign was performed (May 2011-September 2012). All of the monitoring data were shared with the technical stakeholders and decision makers involved in the emergency management. ~~The adopted monitoring system~~

provided all of the technical personnel and the local authorities decision makers involved in the post-crisis management activities with a reliable, rapid and easy communication system of the monitoring results, designed in favour of an enhanced understanding of such a critical landslide scenario and an improvement of decision making process. Based on Given the recorded residual deformations, four critical sectors were identified in the monitored scenario; on the basis of the measured cumulated displacements, frequency of activation and geomorphological features. Amongst these sectors Area 3 and in particular Area 4 (recording respectively 960 mm and 2437 mm of total cumulated displacements) were considered the most hazardous for potential debris flow reactivations. The latter areas are in fact located within a steep landslide sector characterized by loose detrital cover, affected by soil erosion and slope-waste deposition (Dismantling sector). The displacement time series of the GB-InSAR measuring points provided information on the landslide kinematics: displacements range from 337 mm (Point 6) to 1476 mm (Point 8). This latter point displays the monitored area's cumulated peak displacements, showing two acceleration periods (middle March 2011 and beginning of November 2011) triggered by intense precipitations, alternating with a more linear trend. The kinematics of the other representative measuring points, is related either to deformations affecting the deposits placed along the steep scarp connected to the main DSGSD (Points 3-4), or to slope waste deposition due to gravity affecting the coarse material infilling the Detachment sector (Points 1-2-5).

The comparison amongst the MCD maps highlighted a first phase of widespread residual displacements (December 2010). In the following period, ground deformation took place in correspondence of limited sectors within Area 4, except for a widespread reactivation recorded in November 2011. The acquired radar data suggest a complex nature of the monitored landslide: its geomorphological features (e.g., rough topography, stepped profile in its upper sector, showing scarps, counterscarps, ridges, trenches and counterslopes, toe bulging) documents the activity of deep-seated long-term deep-seated processes, while the radar data also recorded the wide spectrum of short-term secondary instability phenomena, probably in terms related to erosional-depositional gravitational processes (Detachment sector), and soil erosion/slope-waste deposition (Dismantling sector). Although this latter sector represents the most hazardous area within the landslide phenomena, the displacements therein acting therein during the analysed time span, appear to be related to ephemeral spring erosion located within the loose detrital cover. This suggests that these processes are only the surficial and secondary expression of a more complex deep-seated landslide system.

The monitoring system adopted provided all of the technical personnel and decision-making local authorities involved in the post-crisis management activities with a reliable, rapid and easy communication system of the results of the monitoring campaign. This favoured an enhanced understanding of such a critical landslide scenario (a populated mountainous area particularly devoted to touristic activities), during the post-emergency management activities. The here presented methodology could represent a useful contribution for a better understanding of landslide phenomena and decision making process during the post-emergency management activities in a critical landslide scenario (a populated mountainous area particularly devoted to touristic activities). Furthermore, the methodology could be profitably adapted, modified, and updated in other geological contexts.

Acknowledgements

The GB-InSAR apparatus used in this application was designed and produced by Ellegi s.r.l. and based on the proprietary LiSALAB GB-InSAR technology, derived from the evolution and improvement of LiSA technology

391 | [\(licensed by the Ispra Joint Research Centre of the European Commission\)](#). We also would like to thank the Veneto Soil
392 Defence Regional Direction for providing Lidar and aerial photo data.

393 References

- 394 Abellán, A., Vilaplana, J.M. and Martínez, J.: Application of a long-range terrestrial laser scanner to a detailed rockfall
395 study at Vall de Núria (Eastern pyrenees, Spain), Eng. Geol., 88, 136–148, 2006.
- 396 Agliardi, F., Crosta, G. and Zanchi A.: Structural constraints on deep-seated slope deformation kinematics. Eng. Geol.,
397 59, 1-2, 83-102, 2001.
- 398 Antonello, G., Casagli, N., Farina, P., Leva, D., Nico, G., Sieber, A.J. and Tarchi D.: Ground-based SAR interferometry
399 for monitoring mass movements, Landslides, 1, 21–28, 2004.
- 400 Bamler, R. and Hartl, P.: Synthetic aperture radar interferometry, Inverse Probl., 14, 1–54, 1998.
- 401 Bardi, F., Frodella, W., Ciampalini, A., Bianchini, S., Del Ventisette, C., Gigli, G., Fanti, R., Moretti, S., Basile, G. and
402 Casagli, N.: Integration between ground based and satellite SAR data in landslide mapping: the San Fratello case study,
403 Geomorphology, 223, 45-60, 2014.
- 404 Bardi, F., Raspini, F., Frodella, W., Lombardi, L., Nocentini, M., Gigli, G., Morelli, S., Corsini, A. and Casagli, N.:
405 Monitoring the Rapid-Moving Reactivation of Earth Flows by Means of GB-InSAR: The April 2013 Capriglio
406 Landslide (Northern Appennines, Italy), Remote Sensing, 9(2), 165, 2017a.
- 407 Bardi, F., Raspini, F., Frodella, W., Lombardi, L., Nocentini, M., Gigli, G., Morelli, S., Corsini, A. and Casagli, N.:
408 Remote sensing mapping and monitoring of the Capriglio landslide (Parma Province, northern Italy). In Mikos, M.,
409 Arbanas, Ž., Yin, Y., Sassa, K. (Eds) Advancing culture of living with landslides, Vol 3 - Advances in Landslide
410 Technology, Springer International Publishing, Switzerland, pp 231-238. Doi: 10.1007/978-3-319-53487-9_26, 2017b.
- 411 Bertolaso, G., De Bernardinis, B., Bosi, V., Cardaci, C., Ciolli, S., Colozza, R., Cristiani, C., Mangione, D., Ricciardi,
412 A., Rosi, M., Scalzo, A. and Soddu P.: Civil protection preparedness and response to the 2007 eruptive crisis of
413 Stromboli volcano, Italy, Journal of Volcanology and Geothermal Research, 182, 269–277, 2009.
- 414 [Bossi, G., Crema, S., Frigerio, S., Mantovani, M., Marcato, G., Pasuto A., Schenato L., Marco Cavalli M.: The Rotolon](#)
415 [catchment early-warning system. In: Lollino G et al. \(eds.\), Engineering Geology for Society and Territory. Springer](#)
416 [International Publishing 3: 91-95, 2015. DOI: 10.1007/978-3-319- 09054-2 18.](#)
- 417 Broussolle, J., Kyovtorov, V., Basso, M., Ferraro Di Silvi, E., Castiglione, G., Figueiredo Morgado, J., Giuliani, R.,
418 Oliveri, F., Sammartino, P.F. and Tarchi, D.: MELISSA, a new class of ground based InSAR system. An example of
419 application in support to the Costa Concordia, ISPRS J. Photogramm. Remote Sens, 91, 50–58, 2014.
- 420 Carlà, T., Intrieri, E., Di Traglia, F. and Casagli, N.: A statistical-based approach for determining the intensity of unrest
421 phases at Stromboli volcano (Southern Italy) using one-step-ahead forecasts of displacement time series, Natural
422 Hazards, 84(1), 669-683, 2016.
- 423 Carlà, T., Intrieri, E., Di Traglia, F., Nolesini, T., Gigli, G. and Casagli, N.: Guidelines on the use of inverse velocity
424 method as a tool for setting alarm thresholds and forecasting landslides and structure collapses, Landslides, 14, (2),
425 517–534, 2017.
- 426 Casagli N, Catani F, Del Ventisette C and Luzi G (2010) Monitoring, prediction, and early warning using ground-based
427 radar interferometry. Landslides 7(3):291-301.
- 428 Casagli, N., Frodella, W., Morelli, S., Tofani, V., Ciampalini, A., Intrieri, E., Raspini, F., Rossi, G., Tanteri, L. and Lu,
429 P.: Spaceborne, UAV and ground-based remote sensing techniques for landslide mapping, monitoring and early
430 warning. Geoenvironmental Disasters 4(9) DOI 10.1186/s40677-017-0073-1, 2017a.

431 Casagli, N., Tofani, V., Morelli, S., Frodella, W., Ciampalini, A., Raspini, F., and Intrieri, E.: Remote Sensing
 432 Techniques in Landslide Mapping and Monitoring, Keynote Lecture. In Mikos, M., Arbanas, Ž., Yin, Y., Sassa, K.
 433 (Eds) Advancing culture of living with landslides, Vol 3 – Advances in Landslide Technology, Springer International
 434 Publishing, Switzerland, pp 1-19. doi: 10.1007/978-3-319-53487-9_1, 2017b.
 435 [Casu, F., Manzo, M., Lanari, R. \(2006\). A quantitative assessment of the SBAS algorithm performance for surface](#)
 436 [deformation retrieval from DInSAR data. Remote Sensing of Environment., 102 \(3-4\), 195-210.](#)
 437 Chandler, J.: Effective application of automated digital photogrammetry for geomorphological research, Earth Surface
 438 Processes and Landforms, 24, 51–63, 1999.
 439 Ciampalini, A., Raspini, F., Bianchini, S., Frodella, W., Bardi, F., Lagomarsino, D., Di Traglia, F., Moretti, S., Proietti,
 440 C., Pagliara, P., Onori, R., Corazza, A., Duro, A., Basile, G. and Casagli, N.: Remote sensing as tool for development of
 441 landslide databases: The case of the Messina Province (Italy) geodatabase, Geomorphology, 249, 103-118, 2015.
 442 Ciampalini A, Raspini F, Frodella W, Bardi F, Bianchini S, Moretti S. (2016) The effectiveness of high-resolution
 443 LiDAR data combined with PSInSAR data. Landslides, 13 (2), 399-410.
 444 Confuorto, P., Di Martire, D., Centolanza, G., Iglesias, R., Mallorqui, J.J., Novellino, A., Plank, S, Ramondini, M.,
 445 Thuro, K. and Calcaterra, D.: Post-failure evolution analysis of a rainfall-triggered landslide by multi-temporal
 446 interferometry SAR approaches integrated with geotechnical analysis. Remote Sensing of Environment, 188, 51-72,
 447 2017.
 448 Crosta G.B. (1996) - Landslide, spreading, deep seated gravitational deformation: Analysis, examples, problems and
 449 proposals. Geografia Fisica e Dinamica Quaternaria, 19: 297–313.
 450 Crosta, G.B. and Agliardi, F.: Failure forecast for large rock slides by surface displacement measurements. Canadian
 451 Geotechnical Journal, 40(1), 176–191, 2003.
 452 Cruden, D.M., and Varnes, D.J.: Landslides Types and Processes. In: Turner AK, Schuster RL (eds.), Landslides:
 453 Investigation and Mitigation. Transportation Research Board Special Report 247, National Academy Press, WA, 36–75,
 454 1996.
 455 Del Soldato, M., Segoni, S., De Vita, P., Pazzi, V., Tofani, V., Moretti, S.: Thickness model of pyroclastic soils along
 456 mountain slopes of Campania (southern Italy). In: Aversa et al. (Eds.). Landslides and Engineered Slopes. Experience,
 457 Theory and Practice. Associazione Geotecnica Italiana, Rome, Italy. ISBN:978-1-138-02988-0, 2016
 458 Del Ventisette, C., Intrieri, E., Luzi, G., Casagli, N., Fanti, R. and Leva, D.: Using ground based radar interferometry
 459 during emergency: The case of the A3 motorway (Calabria Region, Italy) threatened by a landslide, Natural Hazards
 460 and Earth System Science, 11(9), 2483-2495, 2011.
 461 De Zanche V., Mietto P. (1981). Review of the Triassic sequence of Recoaro (Italy) and related problems. Rend. Soc.
 462 Geol. It., Padova. 25-28.
 463 Di Traglia, F., Intrieri, E., Nolesini, T., Bardi, F., Del Ventisette, C., Ferrigno, F., Frangioni, S., Frodella, W., Gigli, G.,
 464 Lotti, A., Tacconi Stefanelli, C., Tanteri, L., Leva, D. and Casagli N.: The ground-based InSAR monitoring system at
 465 Stromboli volcano: Linking changes in displacement rate and intensity of persistent volcanic activity, Bulletin of
 466 volcanology, 76(2), 786, 2014a.
 467 Di Traglia F., Nolesini, T., Intrieri, E., Mugnai, F., Leva, D., Rosi, M. and Casagli N.: Review of ten years of volcano
 468 deformations recorded by the ground-based InSAR monitoring system at Stromboli volcano: a tool to mitigate volcano
 469 flank dynamics and intense volcanic activity, Earth-Sci. Rev., 139, 317–335, 2014b.
 470 Di Traglia, F., Battaglia, M., Nolesini, T., Lagomarsino, D. and Casagli N.: Shifts in the eruptive styles at Stromboli in
 471 2010–2014 revealed by ground-based InSAR data, Scientific Reports, 5, 13569, 2015.

472 Fidolini, F., Pazzi, V., Frodella, W., Morelli, S. and Fanti, R.: Geomorphological characterization, monitoring and
 473 modeling of the Monte Rotolon complex landslide (Recoaro terme, Italy), *Engineering Geology for Society and*
 474 *Territory*, 2, 1311-1315. Springer International Publishing, 2015.

475 [Frigerio, S., Schenato, L., Bossi, G., Cavalli, M., Mantovani, M., Marcato, G., Pasuto, A.: A web-based platform for](#)
 476 [automatic and continuous landslide monitoring: The Rotolon \(Eastern Italian Alps\) case study. *Computers &*](#)
 477 [Geosciences 63: 96-105, 2014. DOI: 10.1016/j.cageo.2013.10.015.](#)

478 Frodella, W., Morelli, S., Fidolini, F., Pazzi, V. and Fanti R.: Geomorphology of the Rotolon landslide (Veneto region,
 479 Italy), *Journal of Maps*, 10(3), 394-401, 2014.

480 Frodella, W., Fidolini, F., Morelli, S. and Pazzi, F.: Application of Infrared Thermography for landslide mapping: the
 481 Rotolon DSGDS case study, *Rend. Online Soc. Geol. It.*, 35, 144-147, 2015.

482 Frodella, W., Ciampalini, A., Gigli, G., Lombardi, L., Raspini, F., Nocentini, M., Scardigli, C. and Casagli, N.:
 483 Synergic use of satellite and ground based remote sensing methods for monitoring the San Leo rock cliff (Northern
 484 Italy), *Geomorphology* 264:80-94, 2016.

485 Frodella, W., Morelli, S. and Pazzi, V.: Infrared Thermographic surveys for landslide mapping and characterization: the
 486 Rotolon DSGSD (Norther Italy) case study, *Italian Journal of Engineering Geology and Environment*. Accepted in
 487 press. DOI: 10.4408/IJEGE.2017-01.S-07, 2017.

488 Gigli, G., Frodella, W., Mugnai, F., Tapete, D., Cigna, F., Fanti, R., Intrieri, E. and Lombardi L.: Instability
 489 mechanisms affecting cultural heritage sites in the Maltese Archipelago, *Nat. Hazards Earth Syst. Sci.* 12:1-2, 2012.

490 Gigli, G., Intrieri, E., Lombardi, L., Nocentini, M., Frodella, W., Balducci, M., Venanti, L.D. and Casagli, N.: Event
 491 scenario analysis for the design of rockslide countermeasures, *J. Mt. Sci.*, 11(6), 1521–1530, 2014a.

492 Gigli, G., Frodella, W., Garfagnoli, F., Mugnai, F., Morelli, S., Menna, F. and Casagli, N.: 3-D geomechanical rock
 493 mass characterization for the evaluation of rockslide susceptibility scenarios, *Landslides*, 11(1), 131-140, 2014b.

494 Gigli, G., Morelli, S., Fornera, S., and Casagli, N.: Terrestrial laser scanner and geomechanical surveys for the rapid
 495 evaluation of rock fall susceptibility scenarios. *Landslides*, 11(1), 1-14, 2014c.

496 [Gullà, G., Peduto, D., Borrelli, L., Antronico, L., Fornaro, G.-\(2017\). Geometric and kinematic characterization of](#)
 497 [landslides affecting urban areas: the Lungro case study \(Calabria, Southern Italy\). *Landslides* 14:171–188, 2017.](#)
 498 [doi:10.1007/s10346-015-0676-0.](#)

499 Guzzetti, F., Mondini, A.C., Cardinali, M., Fiorucci, M., Santangelo, M. and Chang, K.T.: Landslide inventory maps:
 500 new tools for an old problem, *Earth Science Reviews*, 112, 1–25, 2012.

501 Intrieri, E., Gigli, G., Mugnai, F., Fanti, R. and Casagli, N.: Design and implementation of a landslide early warning
 502 system, *Engineering Geology*, 147, 124-136, 2012.

503 Intrieri, E., Gigli, G., Casagli, N. And Nadim, F.: Brief communication" Landslide Early Warning System: toolbox and
 504 general concepts", *Natural hazards and earth system sciences*, 13(1), 85-90, 2013.

505 Jaboyedoff, M., Oppikofer, T., Abellán, A., Derron, M.H., Loye, A., Metzger, R. and Pedrazzini, A.: Use of LIDAR in
 506 landslide investigations: a review, *Natural hazards*, 61(1), 5-28, 2012.

507 Lombardi, L., Nocentini, M., Frodella, W., Nolesini, T., Bardi, F., Intrieri, E., Carlà, T., Solari, L., Dotta, G., Ferrigno,
 508 F. and Casagli, N.: The Calatabiano landslide (southern Italy): preliminary GB-InSAR monitoring data and remote 3D
 509 mapping, *Landslides*:1-12, 2017.

510 Lotti, A., Saccorotti, G., Fiaschi, A., Matassoni, L., Gigli, G., Pazzi, V. and Casagli, N.: Seismic monitoring of
 511 rockslide: the Torgiovanetto quarry (Central Apennines, Italy), in: G. Lollino et al. (eds), *Engineering Geology for*

512 Society and Territory – Vol.2, Springer International Publishing, Switzerland, 1537-1540, doi: 10.1007/978-3-319-
513 09057-3_272, 2015.

514 Luzi, G., Pieraccini, M., Mecatti, D., Noferini, L., Guidi, G., Moia, F. and Atzeni, C.: Ground-based radar
515 interferometry for landslides monitoring: atmospheric and instrumental decorrelation sources on experimental data,
516 IEEE Trans. Geosci. Remote Sens, 42(11), 2454–2466, 2004.

517 Luzi, G.: Ground Based SAR Interferometry: a novel tool for geosciences, P. Imperatore, D. Riccio (Eds.), Geoscience
518 and Remote Sensing. New Achievements, InTech, 1-26, 2010.

519 Monserrat, O., Crosetto, M. and Luzi, G.: A review of ground-based SAR interferometry for deformation
520 measurement, ISPRS Journal of Photogrammetry and Remote Sensing 93, 40-48, 2014.

521 Morelli, S., Pazzi, V., Monroy, V. H. G., and Casagli, N.: Residual Slope Stability in Low Order Streams of Anganguero
522 Mining Area (Michoacán, Mexico) After the 2010 Debris Flows. In Mikos, M., Casagli, N., Yin, Y., Sassa, K. (Eds)
523 Advancing culture of living with landslides, Vol 4 – Diversity of landslide forms, Springer International Publishing,
524 Switzerland, pp 651-660. doi: 10.1007/978-3-319-53485-5_75, 2017.

525 [Nicodemo G, Peduto D, Ferlisi S, Maccabiani J.-\(2016\). Investigating building settlements via very high resolution](#)
526 [SAR sensors. In: Bakker J, Frangopol D.M., van Breugel K \(eds\) © 2017Life-cycle of engineering systems: emphasis](#)
527 [on sustainable Civil Infrastructure. Taylor & Francis Group, London, pp 2256–2263, 2016.](#)

528 Nolesini, T., Di Traglia, F., Del Ventisette, C., Moretti, S. and Casagli, N.: Deformations and slope instability on
529 Stromboli volcano: Integration of GBInSAR data and analog modeling, Geomorphology 180, 242-254, 2013.

530 Nolesini T, Frodella W, Bianchini S and Casagli, N.: Detecting Slope and Urban Potential Unstable Areas by Means of
531 Multi-Platform Remote Sensing Techniques: The Volterra (Italy) Case Study, Remote Sensing, 8(9), 746, 2016.

532 Pagliara, P., Basile, G., Cara, P., Corazza, A., Duro, A., Manfrè, B., Onori, R., Proietti, C. and Sansone, V.: Integration
533 of earth observation and ground-based HR data in the civil protection emergency cycle: the case of the DORIS project,
534 in: Pardo-Igúzquiza E, Guardiola-Albert C, Heredia J, Moreno-Merino L, Durán JJ, Vargas-Guzmán JA (Eds.)
535 Mathematics of Planet Earth, Lecture Notes in Earth System Sciences. Springer, Berlin Heidelberg 263–266, 2014.

536 Pazzi, V., Tanteri, L., Bicocchi, G., Caselli, A., D'Ambrosio, M., Fanti, R.: H/V technique for the rapid detection of
537 landslide slip surface(s): assessment of the optimized measurements spatial distribution. In Mikos, M., Tiwari, B., Yin,
538 Y., Sassa, K. (Eds) Advancing culture of living with landslides, Vol 2 – Advances in landslide science, Springer
539 International Publishing, Switzerland, pp 335-343. doi: 10.1007/978-3-319-53498-5_38. 2017a

540 Pazzi, V., Tanteri, L., Bicocchi, G., D'Ambrosio, M., Caselli, A., and Fanti, R.: H/V measurements as an effective tool
541 for the reliable detection of landslide slip surfaces: Case studies of Castagnola (La Spezia, Italy) and Roccalbegna
542 (Grosseto, Italy), Physics and Chemistry of the Earth, 98, 136-153, doi: <http://dx.doi.org/10.1016/j.pce.2016.10.014>,
543 2017b.

544 [Peduto D., Ferlisi S., Nicodemo G., Reale D., Pisciotta G., Gullà G.-\(2017a\). Empirical fragility and vulnerability](#)
545 [curves for buildings exposed to slow-moving landslides at medium and large scales, Landslides, in press, 2017a. DOI :](#)
546 [10.1007/s10346-017-0826-7.](#)

547 [Peduto, D, Nicodemo, G, Maccabiani, J, Ferlisi, S.-\(2017b\). Multi-scale analysis of settlement induced building damage](#)
548 [using damage surveys and DInSAR data: a case study in The Netherlands. Engineering Geology, 218:117–133, 2017b.](#)
549 [doi:10.1016/j.enggeo.2016.12.018.](#)

550 Pieraccini, M., Tarchi, D., Rudolf, H., Leva, D., Luzi, G., Bartoli, G. and Atzeni, C.: Structural static testing by
551 interferometric synthetic radar, NDT and E Intl., 33(8), 565–570, 2000.

552 Pieraccini, M., Casagli, N., Luzi, G., Tarchi, D., Mecatti, D., Noferini, L. and Atzeni, C.: Landslide monitoring by
 553 ground-based radar interferometry: a field test in Valdarno (Italy), *Int J Remote Sens* 24:1385–1391, 2002.
 554 Salvatici, T., Morelli, S., Pazzi, V., Frodella, W. and Fanti, R.: Debris flow hazard assessment by means of numerical
 555 simulations: implications for the Rotolon Creek Valley (Northern Italy), *Journal of Mountain Science*, 14 (4), 636-648,
 556 DOI:10.1007/s11629-016-4197-7, 2017.
 557 Tarchi, D., Ohlmer, E. and Sieber, A.J.: Monitoring of structural changes by radar interferometry, *Res. Nondestruct.*
 558 *Eval.* 9, 213–225, 1997.
 559 Tarchi, D., Casagli, N., Fanti, R., Leva, D., Luzi, G., Pasuto, A., Pieraccini, M. and Silvano, S.: Landslide monitoring
 560 by using ground-based SAR interferometry: an example of application to the Tessina landslide in Italy, *Engineering*
 561 *Geology*, 68, 15-30, 2003.
 562 Tapete, D., Gigli, G., Mugnai, F., Vannocci, P., Pecchioni, E., Morelli, S., Fanti R., and Casagli, N.: Correlation
 563 between erosion patterns and rockfall hazard susceptibility in hilltop fortifications by terrestrial laser scanning and
 564 diagnostic investigations. In: *IEEE International Geoscience and Remote Sensing Symposium. Remote Sensing for a*
 565 *Dynamic Earth*. Munich, Germany, 22-27 July 2012, pp. 4809-4812. ISBN 978-1-4673-1159-5, 2012.
 566 [Tofani, V., Raspini, F., Catani, F., Casagli, N., Persistent scatterer interferometry \(PSI\) technique for landslide](#)
 567 [characterization and monitoring. In: Sassa, K., Canuti, P., Yueping, Y. \(Eds.\), Landslide Science for a Safer](#)
 568 [GeoenvironmentMethods of Landslide Studies 2. Springer International Publishing, pp. 351–357 \(ISBN:](#)
 569 [9783319050492\).](#) 2014.
 570 Zischinsky, U.: *Über sackungen*, *Rock Mech.*, 1(1), 30–52, 1969.
 571 Zhang, Z., Zheng, S. and Zhan, Z.: Digital terrestrial photogrammetry with photo total station, *International Archives of*
 572 *Photogrammetry and Remote Sensing*, Istanbul, Turkey, 232-236, 2004.